

# RELIABLE REJECTION OF MISMATCHING CANDIDATES FOR EFFICIENT ZNCC TEMPLATE MATCHING

Stefano Mattoccia, Federico Tombari, Luigi Di Stefano

Department of Electronics Computer Science and Systems (DEIS)  
Advanced Research Center on Electronic Systems (ARCES)  
Viale Risorgimento 2 - Bologna, Italy  
{stefano.mattoccia, federico.tombari, luigi.distefano}@unibo.it

## ABSTRACT

This paper presents a method that reduces the computational cost of template matching based on the Zero-mean Normalized Cross-Correlation (ZNCC) without compromising the accuracy of the results. A very effective condition is determined at a small and fixed cost that allow to rapidly detect a large number of mismatching candidates with no need to compute the ZNCC score. Then, thanks to the use of an additional set of conditions, the computation of the whole ZNCC function is typically required only for a very small number of candidates. Experimental results demonstrate the effectiveness of our approach.

**Index Terms**— Template matching, ZNCC, cross correlation, fast, exhaustive

## 1. INTRODUCTION AND RELATED WORK

The purpose of template matching is to detect which part of an *image* is most similar to a given *template*. Template matching is widely deployed for tasks such as quality control, defect detection, robot navigation, face and object recognition, edge detection [1]. *Zero-mean Normalized Cross Correlation* (ZNCC) has been successfully employed as a function to measure the degree of similarity between two image patches due to its invariance with regards to affine photometric distortions.

The standard algorithm, or Full-Search (FS), used to perform ZNCC-based template matching simply scans the image and at each point  $(x, y)$  it computes the ZNCC-score between the template vector and the portion of the image centered in  $(x, y)$  having the same size as the template (image *candidate* vector). Then the image coordinates of the global ZNCC maximum locate the candidate most similar to the template. Denoting as  $I$ ,  $I_c$  and  $T$ , respectively, the image, candidate and template vectors, and having each candidate and template the same size  $M \times N$ , the ZNCC function at pixel position  $(x, y)$  is given by:

$$ZNCC(x, y) = \frac{(I_c(x, y) - \mu_{I_c}(x, y)) \circ (T - \mu_T)}{\|I_c(x, y) - \mu_{I_c}(x, y)\| \cdot \|T - \mu_T\|} \quad (1)$$

with  $\mu_{I_c}(x, y)$  and  $\mu_T$  being respectively the mean intensity value computed over  $I_c(x, y)$  and  $T$ ,  $\circ$  representing the dot product between two vectors, and the two terms at the denominator being respectively the  $L_2$  norm of zero-mean image candidate and zero-mean template vectors. Hereinafter the numerator of (1) will be referred to as  $\eta(x, y)$ .

The FS algorithm turns out to be an expensive task: even if incremental techniques [2], [3] can be adopted to efficiently compute for each point the image candidate mean values and norms in (1), the complexity of  $\eta(x, y)$  is still of the order of  $O(WHMN)$ . A common alternative [4] computes the cross-correlation in the frequency domain by means of the well-known Fast Fourier Transform (FFT), yielding a complexity of the order of  $O(WH \log_2(WH))$ . This approach is exhaustive, i.e. it guarantees to yield exactly the same results as the FS, and turns out to be faster than the FS as the template size approaches the image size and with large templates and images [4].

Another exhaustive approach aimed at speeding up ZNCC-based template matching is the *Zero-mean Bounded Partial Correlation* (ZBPC) technique [5]. This method relies on two computationally efficient upper-bounding functions for  $\eta(x, y)$ ,  $\beta'_{ZBPC}(x, y)$  and  $\beta''_{ZBPC}(x, y)$ , that allow for rapidly pruning mismatching candidates by testing:

$$\frac{\min(\beta'_{ZBPC}(x, y), \beta''_{ZBPC}(x, y))}{\|I_c(x, y) - \mu_{I_c}(x, y)\| \cdot \|T - \mu_T\|} \leq ZNCC_{max} \quad (2)$$

with  $ZNCC_{max}$  being the ZNCC maximum found among previously evaluated candidates. If (2) holds then the current candidate is guaranteed not to be the global maximum and ZNCC computation need not being carried out. Nevertheless, since the computation of both  $\beta'_{ZBPC}(x, y)$  and  $\beta''_{ZBPC}(x, y)$  involves calculating a partial cross-correlation term on a subset of template and candidate vectors (i.e. on  $n_{ZBPC}$  rows), then the speed-ups yielded by ZBPC on FS are upper-bounded by  $\frac{N}{n_{ZBPC}}$ .

Moreover, very recently a fast exhaustive scheme for ZNCC-based block matching was proposed in [6]. By determining a monotonically decreasing equivalent expression of

(1), a Partial Distortion Elimination [7] approach is applied in order to safely terminate the computation of ZNCC as soon as it gets below  $ZNCC_{max}$ .

In the next section a novel fast exhaustive technique, known as *Zero-mean Enhanced Bounded Correlation* (ZEBC), is proposed. This technique aims at improving the ZBPC algorithm and it is inspired by [8]. The two main novelties with respect to ZBPC are represented by the use of two bounding functions which do not require any partial cross-correlation term computation at all and which can be demonstrated being tighter to  $\eta(x, y)$  than  $\beta'_{ZBPC}(x, y)$  and  $\beta''_{ZBPC}(x, y)$ , and by the definition of an additional set of increasingly tighter bounding functions.

## 2. THE ZEBC ALGORITHM

We now devise two novel bounding functions,  $\beta'(x, y)$  and  $\beta''(x, y)$ , which allow to rapidly detect mismatching candidates without the need to compute any partial correlation term. By means of a partitioning scheme similar to that deployed in [8], each candidate and template vectors are subdivided into  $r$  non-overlapping rectangular regions  $R_1, \dots, R_r$  of size  $M \times n$ , with  $n = \frac{N}{r}$ . We will refer to  $I_{c,t}(x, y)$  and  $T_t$  as, respectively, the candidate and template subvectors corresponding to region  $R_t$ , and to  $A_t$  as their cardinality (i.e. the number of pixel in each region,  $A_t = n \cdot M$ ). Then,  $\eta(x, y)$  can be seen as the sum of  $r$  partial terms  $\eta_t(x, y)$  each one computed on its corresponding region  $R_t$ :

$$\eta(x, y) = \sum_{t=1}^r \eta_t(x, y) \quad (3)$$

where:

$$\eta_t(x, y) = (I_{c,t}(x, y) - \mu_{I_{c,t}}(x, y)) \circ (T_t - \mu_{T_t}) \quad (4)$$

By means of the application of the Cauchy-Schwarz inequality on (4) we can devise an upper-bound for term  $\eta_t(x, y)$ :

$$\begin{aligned} \beta'_t(x, y) &= \|I_{c,t}(x, y) - \mu_{I_{c,t}}(x, y)\| \cdot \|T_t - \mu_{T_t}\| = \\ &= \sqrt{\|T_t\|^2 + A_t \cdot \mu_{T_t} (\mu_{T_t} - 2 \cdot \mu_{T_t})} \cdot \\ &\cdot \sqrt{\|I_{c,t}\|^2 + A_t \cdot \mu_{I_{c,t}} (x, y) (\mu_{I_{c,t}} - 2 \cdot \mu_{I_{c,t}})} \quad (5) \end{aligned}$$

All terms in  $\beta'_t(x, y)$  relative to the image candidate can be efficiently computed by means of incremental techniques such as [2], [3], while the others, relative to the template, can be computed once for all at start-up.

Additionally, equation (4) can be algebraically manipulated as follows:

$$\begin{aligned} \eta_t(x, y) &= I_{c,t} \circ T_t + \\ + A_t (\mu_{I_{c,t}}(x, y) \cdot \mu_{T_t} - \mu_{T_t} \cdot \mu_{I_{c,t}}(x, y) - \mu_{T_t} \cdot \mu_{I_{c,t}}(x, y)) \quad (6) \end{aligned}$$

Hence, by applying the Cauchy-Schwarz inequality on the cross-correlation between  $I_{c,t}, T_t$  term in (6) we get an additional upper-bound for  $\eta(x, y)$ :

$$\begin{aligned} \beta''_t(x, y) &= \|I_{c,t}\| \cdot \|T_t\| + \\ + A_t (\mu_{I_{c,t}}(x, y) \cdot \mu_{T_t} - \mu_{T_t} \cdot \mu_{I_{c,t}}(x, y) - \mu_{T_t} \cdot \mu_{I_{c,t}}(x, y)) \quad (7) \end{aligned}$$

Though different from  $\beta'_t(x, y)$ , also this term can be computed very efficiently, partly at start-up and partly by means of incremental schemes. It is worth pointing out that, since both  $\beta'_t(x, y)$  and  $\beta''_t(x, y)$  are computed on the same region  $R_t$ , and since all regions are equally sized, their calculation requires a reduced number of incremental scheme instances, with benefits for what concerns efficiency and memory requirements. Moreover, their computational complexity is independent from image and template sizes.

Thus, we propose a very effective upper-bound for  $\eta(x, y)$  by choosing, for each region  $R_t$ , the term between  $\beta'_t(x, y)$  and  $\beta''_t(x, y)$  that better approximates  $\eta_t(x, y)$ :

$$\beta^B(x, y) = \sum_{t=1}^r \min(\beta'_t(x, y), \beta''_t(x, y)) \quad (8)$$

By comparing (3) and (8) it is easy to infer the bounding property of  $\beta^B(x, y)$ . Hence, for each candidate  $\beta^B(x, y)$  can be used to reliably detect mismatching candidates previously to the computation of the ZNCC term. If condition

$$\frac{\beta^B(x, y)}{\|I_c(x, y) - \mu_{I_c}(x, y)\| \cdot \|T - \mu_T\|} < ZNCC_{max} \quad (9)$$

is verified, then candidate  $I_c(x, y)$  is guaranteed not to be the global maximum and its ZNCC score does not need to be computed.

For the sake of efficiency, since the computation of  $\beta^B(x, y)$  requires the computation of both  $\beta'_t(x, y)$ ,  $\beta''_t(x, y)$  terms on all regions, based on experimental evidence we suggest to compute first

$$\beta''(x, y) = \sum_{t=1}^r (\beta''_t(x, y)) \quad (10)$$

and then to use it to detect a first set of mismatching candidates. The computation of (8) is carried out only for those candidates that are not rejected by means of (10). Though experimentally it seemed more favourable to choose  $\beta''_t(x, y)$  rather than  $\beta'_t(x, y)$  as the bounding terms to be computed first, a deeper study concerning a more advanced scheme aimed at exploiting these terms more effectively is currently under development.

Now, for all candidates not rejected by means of either (8) or (10) we propose to refine the search for mismatching candidates by means of a set of increasingly tighter bounding functions. First, a bounding function can be determined

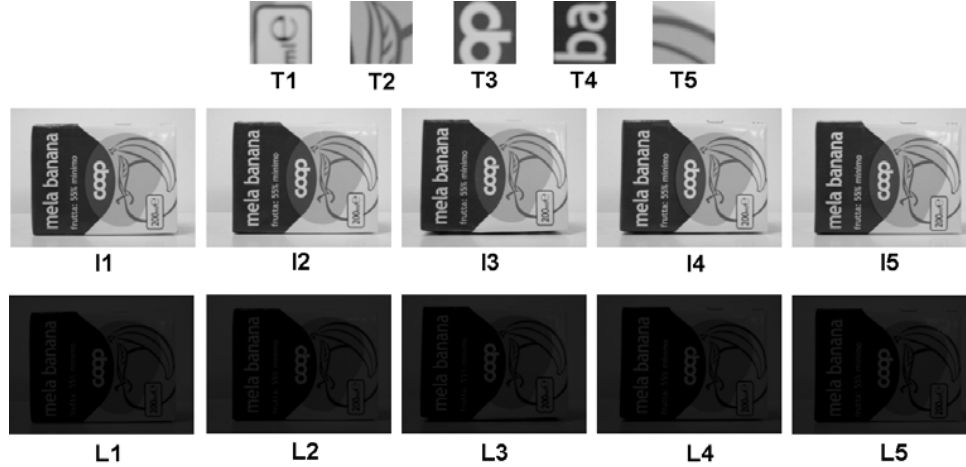


Fig. 1. Dataset used for the experimental results

by substituting in  $\beta^B(x, y)$  the bounding term computed on region  $R_1$  with its corresponding  $\eta_1(x, y)$  term:

$$\gamma^1(x, y) = \eta_1(x, y) + \sum_{t=2}^r \min(\beta'_t(x, y), \beta''_t(x, y)) = \beta^B(x, y) - \min(\beta'_1(x, y), \beta''_1(x, y)) + \eta_1(x, y) \quad (11)$$

where the right hand term in (11) shows how to efficiently compute  $\gamma^1(x, y)$  from  $\beta^B(x, y)$ .  $\gamma^1(x, y)$  represents a tighter approximation of  $\eta(x, y)$  compared to  $\beta''(x, y)$  and  $\beta^B(x, y)$ , though computationally more expensive, hence can be used to classify as mismatching those candidates which were previously not rejected by  $\beta''(x, y)$  and  $\beta^B(x, y)$ .

Following this approach, by substituting at each step the current bounding term with its corresponding  $\eta_t(x, y)$  term, up to  $r - 1$  additional upper bounding functions can be overall deployed for candidate rejection, that is  $\gamma^1(x, y) \cdots \gamma^{r-1}(x, y)$ , the last one being:

$$\gamma^{r-1}(x, y) = \gamma^{r-2}(x, y) - \min(\beta'_{r-1}(x, y), \beta''_{r-1}(x, y)) + \eta_{r-1}(x, y) \quad (12)$$

If not even  $\gamma^{r-1}(x, y)$  is able to reject the current candidate, then the computation of the ZNCC is completed by calculating  $\eta_r(x, y)$ .

It is worth pointing out that similarly to ZBPC, also ZEBBC would benefit of the use of a proper strategy to initialize  $ZNCC_{max}$  with an initial guess aimed at increasing the efficiency of the bounding functions applied. Hence, we propose to use the same coarse-to-fine strategy adopted in [5]. It is worth pointing out that this initialization strategy can not violate the exhaustivity of the search, since the initialized ZNCC maximum can never be higher than the real maximum. Thus, ZEBBC is always FS-equivalent.

### 3. EXPERIMENTAL RESULTS

In this section we propose an experimental evaluation aimed at assessing the benefits brought in by the proposed method, ZEBBC, by comparing it to the other state-of-the-art fast exhaustive template matching approaches. As a benchmark for evaluation we propose a typical quality assessment setup, where 5 templates,  $T1 \cdots T5$  of size  $64 \times 64$  were uniformly extracted from a reference image of a product item and then searched in the images of different items, as if on a production belt. In particular, 5 different images of as many items,  $I1 \cdots I5$ , are used, each one sized  $640 \times 480$ . This dataset is shown in Fig. 1.

As for the comparison, ZEBBC is tested against FS, FFT-based and ZBPC. FS deploys incremental calculation schemes to efficiently compute the candidate norms and mean values in (1). ZBPC parameter  $\frac{n_{ZBPC}}{N}$  was optimally tuned to 0.07. As for FFT, we used the implementation proposed in well-known OpenCV library, optimized with SIMD instructions. For what regards ZEBBC, parameter  $r$  was set to 8. In addition, for fairness of comparison, when tested against the FFT also for ZEBBC a SIMD optimization is used. Finally, the sampling factor  $k$  used for the initial multi-resolution scheme [5] employed by both ZBPC and ZEBBC was set to 4.

Table 1 reports the speed-ups (ratios of measured execution times) of the ZEBBC algorithm against, from left to right, FS, ZBPC and FFT, obtained on a PC running Linux with 3.06 GHz clock AMD CPU. The last row of the table reports the mean speed-up reported by ZEBBC against the three algorithms. From the table it can be noted that ZEBBC is always able to notably speed-up the FS algorithm, speed-ups ranging between 11.5 and 28.5. Moreover, ZEBBC is always faster than ZBPC and FFT, mean speed-ups being respectively 2.1 and 2.5. It is also worth noting that ZEBBC, despite being a data-dependent technique, showed a rather limited range of variations of the measured speed-ups.

**Table 1.** Measured speed-ups: ZEBC Vs. FS, ZBPC and FFT-based algorithms.

	ZEBC vs FS					ZEBC vs ZBPC					ZEBC vs FFT				
	I1	I2	I3	I4	I5	I1	I2	I3	I4	I5	I1	I2	I3	I4	I5
<b>T1</b>	17.2	15.1	14.7	24.5	23.5	1.5	1.3	1.5	2.1	2.1	2.4	2.1	2.1	3.0	2.9
<b>T2</b>	15.2	15.6	11.6	11.5	13.8	1.4	1.4	2.3	2.3	1.4	2.2	2.3	1.8	1.8	2.0
<b>T3</b>	19.3	21.4	17.7	22.8	15.9	1.7	1.8	1.6	2.0	1.4	2.6	2.8	2.4	2.9	2.2
<b>T4</b>	14.3	15.4	19.0	17.5	15.7	1.3	1.4	1.6	1.6	1.4	2.1	2.2	2.6	2.4	2.2
<b>T5</b>	27.7	27.8	28.5	28.0	12.4	3.9	4.9	3.1	3.4	3.9	3.3	3.4	3.4	3.4	1.8
<b>Mean</b>	18.6					2.1					2.5				

**Table 2.** Measured speed-ups on dataset affected by affine photometric distortions.

	ZEBC vs FS					ZEBC vs ZBPC					ZEBC vs FFT				
	L1	L2	L3	L4	L5	L1	L2	L3	L4	L5	L1	L2	L3	L4	L5
<b>T1</b>	13,7	12,8	12,2	19,7	18,2	1,3	1,2	1,3	1,8	1,7	2,0	1,9	1,9	2,7	5,3
<b>T2</b>	12,7	13,4	10,6	10,4	11,8	1,3	1,3	2,2	2,2	1,3	2,0	2,0	1,7	1,7	1,9
<b>T3</b>	15,2	16,7	14,1	17,5	19,1	1,4	1,5	1,3	1,6	0,8	2,2	2,4	2,1	2,5	2,0
<b>T4</b>	8,5	9,1	9,5	10,6	10,8	3,6	2,4	2,5	1,7	1,9	1,4	1,5	1,5	1,8	1,7
<b>T5</b>	23,2	23,0	23,6	23,6	10,4	3,4	4,1	2,8	3,0	3,3	3,0	3,0	2,0	3,1	1,7
<b>Mean</b>	14,8					2,0					2,2				

In addition, we also propose a further experiment where synthetic illumination distortions are applied between images and templates. In particular, all images are transformed according to an affine mapping function ( $gain = 0.25$ ,  $bias = -20$ ), as shown in Fig. 1, images  $L1 \dots L5$ . This is motivated by the fact that ZNCC is typically employed in those cases where photometric distortions which can be assimilated to affine illumination changes are present between image and template, since ZNCC is invariant to this kind of transformations. Table 2 shows the speed-ups reported with this dataset by ZEBC against FS, ZBPC, FFT. By comparing the two tables it can be noted that, despite the notable distortions affecting the images, ZEBC is always the fastest algorithm, its speed-ups being lightly affected by the introduced distortions. From a theoretical point of view this can be explained since the effectiveness of all bounding functions applied by ZEBC, though not demonstrated here for lack of space, is robust to the presence of constant multiplicative and additive factors within  $I$  and  $T$ . Hence the decrease of speed-ups between the two tables has to be mainly ascribed to the distortions due to intensity quantization and saturation arising when such kind of synthetic transformation is applied.

#### 4. CONCLUSIONS AND FUTURE WORK

We have presented ZEBC, a FS-equivalent technique to speed-up ZNCC-based template matching. Experimental results demonstrate that ZEBC is currently faster compared to the other FS-equivalent template matching approaches. Future work is aimed at comparing ZEBC with the very recent approach proposed in [6] within a template matching

framework.

#### 5. REFERENCES

- [1] A. Goshtasby, *2-D and 3-D image registration for medical, remote sensing and industrial applications*, Wiley, 2005.
- [2] M. Mc Donnell, "Box-filtering techniques," *Computer Graphics and Image Proc.*, vol. 17, pp. 65–70, 1981.
- [3] F. Crow, "Summed-area tables for texture mapping," *Computer Graphics*, vol. 18, no. 3, pp. 207–212, 1984.
- [4] J.P. Lewis, "Fast template matching," in *Proc. Conf. on Vision Interface*, May 1995, pp. 120–123.
- [5] L Di Stefano, S Mattocchia, and F Tombari, "Zncc-based template matching using bounded partial correlation," *Patt. Rec. Letters*, vol. 26, no. 14, 2005.
- [6] A. Mahmood and S Khan, "Early termination algorithms for correlation coefficient based block matching," in *Proc. ICIP*, 2007, vol. 2, pp. 469–472.
- [7] C.D. Bei and R.M. Gray, "An improvement of the minimum distortion encoding algorithm for vector quantization," *IEEE Trans. Comm.*, vol. 33, pp. 1132–1133, 1985.
- [8] S. Mattocchia, F. Tombari, and L. Di Stefano, "Fast full-search equivalent template matching by enhanced bounded correlation," *IEEE Trans. Image Processing*, vol. 17, no. 4, pp. 538–538, 2008.